Journal of Integrative Neuroscience, Vol. 3, No. 2 (2004) 227–244
© Imperial College Press
Imperial College Press
www.icpress.co.uk

Research Report

SCALING LAWS FOR MYELINATED AXONS DERIVED FROM AN ELECTROTONIC CORE-CONDUCTOR MODEL

PETER J. BASSER
National Institutes of Health
13 South Drive, Bldg. 13, Rm. 3W16
Bethesda, MD 20892-5772, USA
pjbasser@helix.nih.gov

Received 29 February 2004
Accepted 24 April 2004

A macroscopic cable equation, which describes the passive linear ("electrotonic") response of a myelinated axon, was previously derived from a segmented cable equation using Keller's two-space homogenization method [Basser, PJ, *Med. and Biol. Comput.*, 1993, Vol. 31, pp. S87–S92]. Here we use the space and length constants of this averaged cable equation to predict classical scaling laws that govern relationships among the inner and outer diameters of the axon's myelin sheath and the distance separating adjacent nodes of Ranvier. These laws are derived by maximizing the characteristic speed of an electrical disturbance along the axon, i.e., the ratio of the characteristic length and the characteristic time constants of the macroscopic cable, subject to the constraint that the nodal width is constant. Using this result, it is also possible to show that all myelinated axons are equally fault tolerant. No free parameters were used in this analysis; all variables and physical constants used in these calculations were taken from published experimental data.

Keywords: Scaling; axon; myelin; cable; model; equation; two-space method; homogenization.

1. Introduction

In 1951, Rushton explained that the inner and outer diameters of an axon's myelin sheath maintain a fixed proportion independent of axon size in order to maximize the space constant of the myelinated portion of the axon for any given outer diameter [1]. Rushton also introduced the notion that corresponding parts of different myelinated axons are isopotential (i.e., the principle of "corresponding states") to explain why the ratio of the distance between adjacent nodes of Ranvier and the outer diameter of the myelin sheath is constant among axons of different sizes. However, Rushton did not derive this constant of proportionality [1].

FitzHugh [2] and Goldman [3] showed that the principle of corresponding states implied that cable equations describing the dynamics behavior of myelinated axons

are dimensionally similar. In particular, dimensionless groups appearing within them must have the same value for myelinated axons of different sizes. This argument finds its basis in the principle of "dynamic similarity" that has been widely used in fluid dynamics.

An alternative approach, suggested by FitzHugh, is to derive Rushton's scaling relationships from a maximum principle, by supposing that the myelinated axon optimizes certain desirable attributes, such as its conduction velocity, fault tolerance and energetic efficiency [2]. However FitzHugh did not attempt to construct such a multi-attribute objective function. Below, it is shown that by maximizing a simple objective function — the characteristic speed of a weak electrical disturbance along a macroscopic cable — one can derive Rushton's scaling relationships. A prerequisite, however, is to obtain the form of a cable equation that describes the spatial and temporal evolution of the electrical potential and current distribution along a segmented myelinated axon, which predicts its passive electrical response.

This paper has two purposes: to recapitulate expressions for the macroscopic space constant and time constant of a myelinated axon, and to use these to derive several useful scaling laws of the axon without invoking Rushton's principle of corresponding states. Accordingly, this paper is divided into two main parts. In Section 2, we review how the two-space method of Keller [4] can be used to derive a homogenized cable equation that describes the sub-threshold dynamic behavior of a myelinated axon. In Section 3, we use the expressions for the space and time constants of the composite passive electrical cable to derive Rushton's scaling laws from the physically reasonable proposition that an optimally designed myelinated axon maximizes the characteristic speed of a weak electrical disturbance.

2. Motivation for the Two-Space Method

Peripheral myelinated axons conduct electrical impulses toward muscles from the brain or spinal cord (motor fibers) or transmit sensory impulses toward the brain or spinal cord (afferent fibers) [5]. A schematic diagram of a myelinated axon is given in Fig. 1. It contains segments with active membranes called nodes of Ranvier that are each δ wide and spaced a distance L apart. The nodes are joined by membranes insulated by myelin sheaths.

A neurologist is often interested in measuring macroscopic properties of axons *in vivo*, such as their conduction velocity [6], or related physical quantities such as the current that must flow through an inductive coil [7] or trans-cutaneous electrode sufficient to elicit stimulation [8]. To meet these needs, models have been proposed to explain how the applied electric field distributions induced by current-carrying coils [9, 10] or transcutaneous electrodes [8, 11, 12] stimulate myelinated nerves. The characteristic length of these applied electric fields is usually on the order of the diameter of the stimulating coil or the electrode separation, which are typically a few centimeters [10]. The characteristic dimension of the internode is at most 0.2 cm, while the characteristic dimension of the node of Ranvier is its width, taken to be 0.00015 cm [13]. Because of the more than 10,000-fold difference between the largest

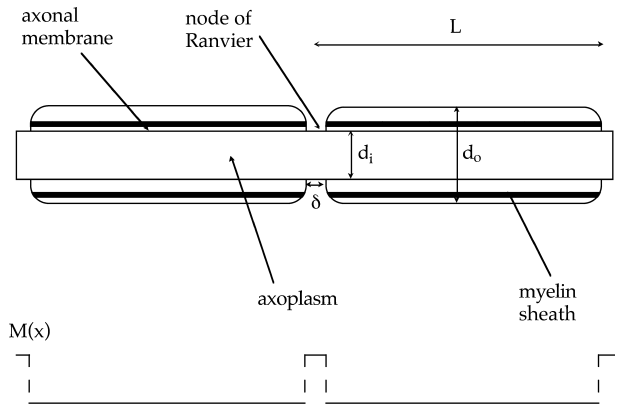

Fig. 1. A schematic diagram of a myelinated axon. The axonal membrane contains active regions, nodes of Ranvier, which are joined by passive segments insulated by myelin. Nodes are spaced a distance L apart and are δ wide. The outer diameter of the axon is d_o; its inner diameter d_i.

and smallest length scales, it is imprudent to describe the effect of macroscopic applied electric fields on an axon using a microscopic length scale. This would be akin to using a micrometer to measure the dimensions of a room. To address this problem, we have used the two-space perturbation method of Keller [4, 14] to develop a macroscopic description of a composite cable equation of a myelinated axon that appropriately balances the contributions from the nodal membranes and the insulated myelinated portions. This approach provides a macroscopic description of the current and electrical potential distribution along the axon, while preserving the microscopic electrical properties and dimensions as parameters within the governing equation [15].

Although the homogenized cable model is valid when the radius of the current-carrying coil or the separation between stimulating electrodes is much greater than the separation between nodes of Ranvier, it is also valid for sub-threshold nodal stimulation [16].

Previously, this averaged or homogenized cable equation was used to predict the response of myelinated nerves to electromagnetic and electrical stimulation in the subthreshold regime. It was also shown that this cable equation adequately predicted threshold behavior when it was compared with numerical solutions of the non-linear Hodgkin-Huxley cable equations adapted to a myelinated axon [17]. In particular, it was shown that a strength-duration curve for the myelinated axon could be predicted using the average, passive macroscopic cable model [17].

2.1. *Composite cable equation of a myelinated axon*

An equation of a segmented cable is written in a new form, which makes it amenable to simplification, by the two-space method:

$$\frac{\partial^2 V}{\partial x^2} = (1 - M(x)) \left(\frac{\tau_m}{\lambda_m^2} \frac{\partial V}{\partial t} + \frac{V}{\lambda_m^2} \right) + M(x) \left(\frac{\tau_n}{\lambda_n^2} \frac{\partial V}{\partial t} + \frac{V}{\lambda_n^2} + \Phi_{\text{ion}} \right) + f(x, t). \tag{1}$$

Above, $V = V(x,t)$ is the distribution of transmembrane potential along the composite cable with respect to the axon's rest potential (which is assumed to be uniform and equal in both domains), and $\tau_m, \lambda_m, \tau_n$, and λ_n are the myelin and nodal time constants and space constants, respectively. The function, $M(x)$, contains anatomical information about the axon. As shown in Figure 1, $M(x)$ is a train of boxcars that are δ wide and spaced L apart. It can be synthesized by superposing Heaviside functions of unit height, $H(x)$, i.e.,

$$M(x) = \sum_{n=-\infty}^{n=\infty} \left[H\left(x - nL + \frac{\delta}{2}\right) - H\left(x - nL - \frac{\delta}{2}\right) \right]. \tag{2}$$

The function, $M(x)$, determines the transmembrane current at each value of x. For example, when x lies within a node of Ranvier, $M(x) = 1$; the transmembrane current arises from the second and third terms on the right hand side of Eq. (1). Conversely, when x lies within the internodal region, $M(x) = 0$; the transmembrane current arises from the first and third term on the right hand side of Eq. (1).

The conditions of continuity of axial current and transmembrane potential at the boundaries between nodal and myelinated elements are implicit in Eqs. (1) and (2), unlike FitzHugh's [18] and Andrietti and Bernadini's [16] segmented cable equations. For completeness, the contribution of the active transmembrane ionic current, Φ_{ion}, is included in Eq. (1), but hereafter is set to zero because it can be shown not to contribute significantly to the transmembrane current in the subthreshold regime. The cable equation, Eq. (1), also contains a source term, f(x, t). For electromagnetic stimulation of a nerve fiber, $f(x,t) = \partial \varepsilon_x(x,t)/\partial x$ where $\varepsilon_x(x,t)$ is the component of the net applied electric field along the direction of the nerve fiber axis [10, 15]. For electrical stimulation, $f(x,t) = -\partial^2 V_e(x,t)/\partial^2 x$ where $V_e(x,t)$ is the applied extracellular potential distribution [8, 12, 19]. The source of transmembrane potential acts in both the nodal and internodal regions.

In Eq. (1), the space constant of the internodal region, λ_m, is defined as

$$\lambda_m = d_i \sqrt{\frac{\rho_m}{8\rho_a} \ln\left(\frac{d_o}{d_i}\right)} \tag{3}$$

and the time constant, τ_m, by

$$\tau_m = \varepsilon_0 \kappa_m \rho_m, \tag{4}$$

where ρ_m and ρ_a are the resistivities of myelin and axoplasm, respectively; κ_m is the dielectric constant of myelin; ε_0 is the permittivity *in vacuo*; d_o is the outer diameter of the myelin sheath; and d_i is the inner diameter of the myelin sheath.

Analogously, the space constant of the node, λ_n, is defined by

$$\lambda_n = d_i \sqrt{\frac{\rho_n}{8\rho_a} \ln\left(\frac{d_i + 2h}{d_i}\right)} \approx d_i \sqrt{\frac{\rho_n}{8\rho_a} \frac{2h}{d_i}} \tag{5}$$

Table 1.

Physical Variables		
x	distance along the nerve fiber axis	cm
t	time	sec
$V(x,t)$	transmembrane potential	mV
Nerve Model		
E_{Na}	sodium Nernst potential at 37°C	35.35 mV
E_L	leakage Nernst potential at 37°C	−80.01 mV
g_{Na}	sodium conductance	$1,445\ mS/cm^2$
g_L	leakage conductance	$128\ mS/cm^2$
c_n	nodal capacitance per unit area	$2.5\,\mu F/cm^2$
ρ_a	resistivity of axoplasm	5.47×10^{-2} kOhm-cm
ρ_m	resistivity of myelin	7.4×10^5 kOhm-cm
κ_m	dielectric constant of myelin	7
ρ_n	resistivity of nodal membrane	6.9×10^5 kOhm-cm
κ_n	dielectric constant of nodal membrane	7
ε_0	permittivity of a vacuum	$8.85 \times 10^{-8}\,\mu F/cm$
δ	width of node of Ranvier	1.5×10^{-4} cm
d_i	inner diameter of axon membrane	2 to 20×10^{-4} cm
d_o	outer diameter of myelin sheath	3 to 30×10^{-4} cm
h	thickness of the nodal membrane	5×10^{-7} cm
L	distance between nodes of Ranvier	3 to 30×10^{-2} cm

where h is the thickness of the nodal membrane, which is of the order of nanometers. The time constant, τ_n, is given by

$$\tau_n = \varepsilon_0 \kappa_n \rho_a, \tag{6}$$

where κ_n is the dielectric constant of nodal membrane. An axon with $d_o = 0.0014$ cm and $d_i = 0.00085$ cm, and material parameters given in Table 1, has the following space and time constants: $\lambda_m = 0.55$ cm, $\tau_m = 460\,\mu s$, $\lambda_n = 0.0077$ cm, $\tau_n = 61\,\mu s$.

2.2. *Deriving a macroscopic cable equation of a composite myelinated axon*

Keller illustrated the use of the two-space method [4] to calculate the effective thermal conductivity of a composite medium from the steady-state heat equation. Here, it is used to derive a time-varying macroscopic cable equation of a composite, myelinated axon. In Keller's example [4], the thermal conductivity is varied as a function of axial length while the transverse conductivity remained constant. In this example, the axial electrical conductivity is constant but the membrane impedance varies as a function of axial distance.

First, two length scales are identified: x', which describes the large-scale variations on the order of the applied field, and $y(x') = x'/\varepsilon$, which describes variations on the scale of the nodal width, δ. For example, in electromagnetic stimulation, $0 < \varepsilon \sim O(10^{-5}) \ll 1$ for an axon with an outer diameter of 0.001 cm. The

transmembrane potential is assumed to depend upon both of these length scales. Equation (1) can then be rewritten in the following form:

$$\frac{\partial^2 V(x', \frac{x'}{\varepsilon}, t)}{\partial x^2} = h\left(x', \frac{x'}{\varepsilon}, t\right) = h(x', y(x'), t). \tag{7}$$

If x' and $y(x')$ are treated as independent variables, then the chain rule requires that the partial differentiation operator with respect to x be replaced by the following operator in x' and y:

$$\frac{\partial}{\partial x} \equiv \frac{\partial}{\partial x'} + \frac{1}{\varepsilon}\frac{\partial}{\partial y}. \tag{8}$$

Therefore Eq. (7) above becomes:

$$\left(\frac{\partial^2}{\partial x'^2} + \frac{2}{\varepsilon}\frac{\partial}{\partial y}\frac{\partial}{\partial x'} + \frac{1}{\varepsilon^2}\frac{\partial^2}{\partial y^2}\right) V(x', y, t) = h(x', y, t). \tag{9}$$

The transmembrane potential is expanded as a power series in the perturbation parameter, ε:

$$V(x', y, t, \varepsilon) = v_0(x', y, t) + v_1(x', y, t)\varepsilon + v_2(x', y, t)\varepsilon^2 + O(\varepsilon^3)\ldots \tag{10}$$

Each function $v_i(x', y, t)$ is assumed to be bounded. Substituting Eq. (10) into Eq. (9) and grouping terms with like powers of ε, we get:

$$\varepsilon^{-2}\text{:}\ \frac{\partial^2 v_0(x', y, t)}{\partial y^2} = 0 \tag{11a}$$

$$\varepsilon^{-1}\text{:}\ \frac{\partial}{\partial y}\frac{\partial v_0(x', y, t)}{\partial x'} + \frac{\partial^2 v_1(x', y, t)}{\partial y^2} = 0 \tag{11b}$$

$$\varepsilon^{0}\text{:}\ \frac{\partial^2 v_0(x', y, t)}{\partial x'^2} + 2\frac{\partial}{\partial y}\frac{\partial v_1(x', y, t)}{\partial x'} + \frac{\partial^2 v_2(x', y, t)}{\partial y^2} = h(x', y, t). \tag{11c}$$

Integrating the ε^{-2} equation, Eq. (11a), with respect to y we obtain:

$$v_0(x', y, t) = v_0(x', y_0, t) + (y - y_0)\left.\frac{\partial v_0(x', y, t)}{\partial y}\right|_{y=y_0} \tag{12}$$

where y_0 is an arbitrary constant of integration. Since v_0 is bounded for all values of y and t, including the limit as y approaches infinity, the second term on the right hand side of Eq. (12) must vanish. Therefore the derivative must vanish, i.e.,

$$\left.\frac{\partial v_0(x', y, t)}{\partial y}\right|_{y=y_0} = 0 \tag{13}$$

which implies that

$$v_0(x', y, t) = v_0(x', t). \tag{14}$$

This means that the lowest order term in the perturbation expansion is only a function of the macroscopic length variable and time, but does not depend on the

small scale variable, y. With the help of Eq. (14), integration of the ε^{-1} equation, Eq. (11b), with respect to y yields:

$$v_1(x', y, t) = v_1(x', y_0, t) + (y - y_0) \left. \frac{\partial v_1(x', y, t)}{\partial y} \right|_{y=y_0} . \tag{15}$$

For $v_1(x', y, t)$ to be bounded, we also require that:

$$\left. \frac{\partial v_1(x', y, t)}{\partial y} \right|_{y=y_0} = 0 \tag{16}$$

or

$$v_1(x', y, t) = v_1(x', t) \tag{17}$$

Finally, with the help of Eqs. (14) and (16) integration of the ε^0 equation (Eq. (11c)) with respect to y yields:

$$\frac{1}{y - y_0} \left. \frac{\partial v_2(x', y, t)}{\partial y} \right|_{y_0}^{y} = -\frac{\partial^2 v_0(x', t)}{\partial x'^2} + \frac{1}{y - y_0} \int_{y_0}^{y} h(x, u, t) du \tag{18}$$

where u is a dummy variable. In the limit as y approaches infinity, the term on the left hand side of Eq. (18) vanishes by the assumption of the boundedness of v_2. Therefore, the equation for the lowest order term in the perturbation expansion, Eq. (10), is given by:

$$\frac{\partial^2 v_0(x', t)}{\partial x'^2} = \lim_{y \to \infty} \frac{1}{y - y_0} \int_{y_0}^{y} h(x', u, t) du = < h(x', t) > . \tag{19}$$

The integral in Eq. (19) is the familiar ergodic mean of $h(x', y, t)$ over the small-scale variable, y. Thus, $< h(x', t) >$ no longer explicitly depends upon y. This is the desired simplification: Small-scale variations in nodal impedance have been eliminated by integration although their effect has been preserved.

In the cable model, the function $h(x', y, t)$ in Eq. (7) can be rewritten in terms of x' and y:

$$\begin{aligned} h(x', y, t) = (1 - M(y)) \left(\frac{\tau_m}{\lambda_m^2} \frac{\partial v_0(x', t)}{\partial t} \right) + \frac{v_0(x', t)}{\lambda_m^2} \\ + M(y) \left(\frac{\tau_n}{\lambda_n^2} \frac{\partial v_0(x', t)}{\partial t} \right) + \frac{v_0(x', t)}{\lambda_n^2} + f(x', t), \end{aligned} \tag{20}$$

where

$$M(y) = \sum_{n=-\infty}^{n=\infty} \left[H\left(y - \frac{nL}{\delta} + \frac{1}{2} \right) - H\left(y - \frac{nL}{\delta} - \frac{1}{2} \right) \right]. \tag{21}$$

The function, M, is now expressed in terms of y so that $h(x', y, t)$ is continuously differentiable with respect to x', a requirement of the two-space method [14]. Because $M(y)$ is also periodic, i.e., $M(y) = M(y + L), < h(x', t) >$ in Eq. (19) reduces to:

$$< h(x', t) > = \frac{\delta}{L} \int_{-\frac{L}{2\delta}}^{\frac{L}{2\delta}} h(x', t, u) du \tag{22}$$

After grouping terms in Eqs. (20) and (21), homogenization or spatial averaging results in a macroscopic cable equation for v_0 of the form:

$$\frac{\partial^2 v_0(x', t)}{\partial x'^2} = \frac{\tau}{\lambda^2} \frac{\partial v_0(x', t)}{\partial x'^2} + \frac{v_0(x', t)}{\lambda^2} + f(x', t) \tag{23}$$

in which the effective space and time constants, λ and τ, are functions of the space and time constants of the myelinated and nodal membranes, respectively. These, in turn, are functions of the internodal distance, nodal width, and other microstructural parameters:

$$\lambda = \left[\left(1 - \frac{\delta}{L} \right) \frac{1}{\lambda_{m^2}} + \frac{\delta}{L} \frac{1}{\lambda_{n^2}} \right]^{-\frac{1}{2}} \tag{24}$$

$$\tau = \lambda^2 \left[\left(1 - \frac{\delta}{L} \right) \frac{\tau_m}{\lambda_m^2} + \frac{\delta}{L} \frac{\tau_n}{\lambda_n^2} \right]. \tag{25}$$

Equations (24) and (25) derived above are consistent with formulae for λ and τ obtained from a discrete model of a segmented cable (e.g., [16]).

Although Andrietti and Bernadini [16] showed good agreement between analytical solutions to Eqs. (23), (24), and (25) and numerical solutions of their segmented cable model for both nodal current and transmembrane potential stimuli for a specific set of parameters, they were unable to show that Eqs. (23), (24) and (25) formally approximated their segmented cable equations. Using the two-space method, it was shown previously that Eqs. (23), (24) and (25) are the lowest order approximation to the full segmented cable equation. In principle, the two-space method also permits higher-order terms to be calculated in the perturbation expansion (Eq. (10)) and more importantly, can be extended to include non-linear membrane kinetics.

One goal of this paper is to use the macroscopic space and time constants, λ and τ, above to derive scaling relationships for myelinated axons. Below, λ and τ from Eqs. (24) and (25) are written in terms of d_i, d_o, δ and L, and material constants given in Table 1 for use in the next section:

$$\lambda = 10^3 d_i \left[\frac{8.8}{\ln\left(1 + \frac{1.24\,10^{-6}}{d_i}\right)} \frac{\delta}{L} + \frac{1.18919}{\ln\left(\frac{d_o}{d_i}\right)} \left(1 - \frac{\delta}{L} \right) \right]^{\frac{-1}{2}} \text{cm} \tag{26}$$

$$\tau = \lambda^2 \frac{10^{-8}}{d_i^2} \left[\frac{0.53737}{\ln\left(1 + \frac{1.24\,10^{-6}}{d_i}\right)} \frac{\delta}{L} + \frac{0.547265}{\ln\left(\frac{d_o}{d_i}\right)} \left(1 - \frac{\delta}{L} \right) \right] \text{sec.} \tag{27}$$

For example, an axon with $d_o = 0.0014\,\text{cm}$ and $d_i = 0.00085\,\text{cm}$, and material parameters given in Table 1, has the following macroscopic space and time constants: $\lambda = 0.217\,\text{cm}$ and $\tau = 123\,\mu s$. Note, these equivalent cable parameters are intermediate between the nodal and internodal space and time constants.

3. Derivation of Rushton's Scaling Laws

Rushton [1] proposed scaling relationships for myelinated axons of different diameters, which have since been verified experimentally [3]. One law is that the ratio of the inner and outer diameters of the myelin sheath is constant, i.e.,

$$\frac{d_i}{d_o} = \exp\left(\frac{-1}{2}\right) = 0.6065\ldots. \tag{28}$$

Goldman and Albus [3] argue that this ratio maximizes the myelin space constant, λ_m, with respect to d_i for a fixed d_o. A plot of the normalized myelin space constant, λ_m/d_o vs. the ratio of inner and outer diameters, d_i/d_o is given in Fig. 2. Using Eq. (3), it is easy to verify that the maximum in λ_m/d_o occurs at $d_i/d_o = 0.6065$ for d_o constant. Subsequently, FitzHugh [2] argued that this ratio of inner and outer diameters maximizes the "safety ratio" of an axon for a given outer diameter.

The second of Rushton's scaling laws is that the distance between nodes of Ranvier varies linearly with axon outer diameter. Rushton's data obtained from axons of cats and kittens is replotted in Fig. 3. The node spacing is approximately 87 times the outer diameter [1], i.e.,

$$\frac{L}{d_o} = 87. \tag{29}$$

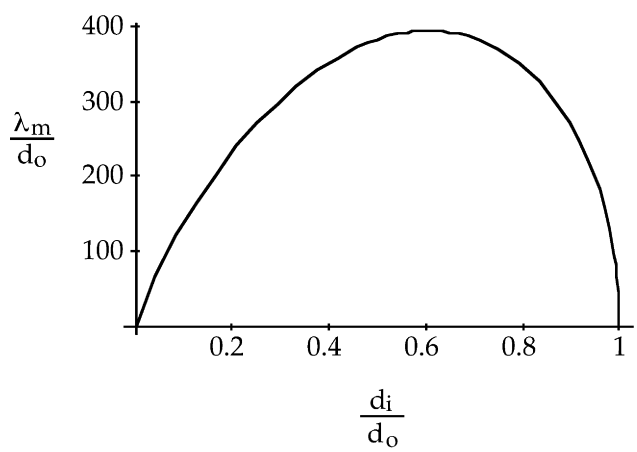

Fig. 2. Space constant of a myelinated membrane normalized by axon outer diameter, λ_m/d_o, vs. the ratio of inner and outer diameters, d_i/d_o, calculated from Eq. (5). The maximum occurs at $d_i/d_o = 0.6065$.

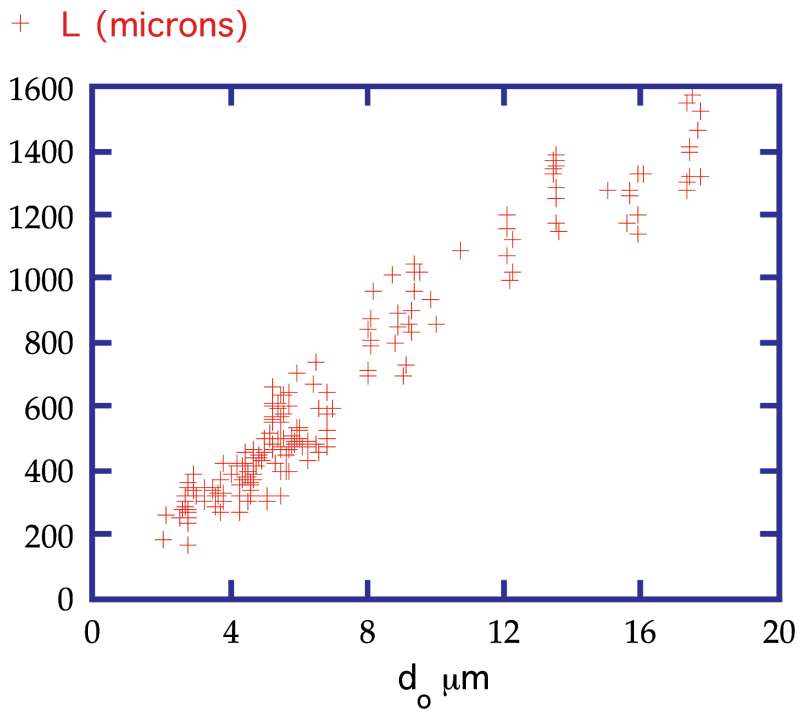

Fig. 3. Outer membrane diameter, d_o, vs. distance between nodes, L, for axons from cats and kittens (replotted from [1]).

This linear relationship does not hold for axons whose diameters are less than 0.0004 cm [1, 20]. Although Rushton argues that L and d_o should be linearly related according to the principle of corresponding states, he does not derive the constant of proportionality. FitzHugh [2] and Goldman [3] also clarified why L is directly proportional to d_o, but do not predict the constant of proportionality. What physical principle could explain this result? It is likely that there are two competing physical effects at work.

One could suppose that the observed value of L maximizes λ for a constant d_o. However, as shown in Fig. 4, $\lambda(d_i, L)/d_o$ increases monotonically with L. Although Fig. 4 is calculated for $d_o = 0.0014$ cm and $\delta = 0.00015$ cm, this result holds for all values of d_o within the physiological range. Therefore, maximizing $\lambda(d_i, L)/d_o$ with respect to L leads to the erroneous conclusion that the optimal node separation is infinite. In addition, because λ_m is independent of L, no optimum exists for λ_m with respect to L.

The membrane time constant, τ, measures the time for the transmembrane potential to reach its steady-state value after small perturbations in current or voltage have been applied [21]. Figure 5 shows a plot of the effective membrane time constant, τ, as a function of the inner diameter of the axon, d_i, and internodal distance, L, for $d_o = 0.0014$ cm and $\delta = 0.00015$ cm using Eq. (26). It is important to

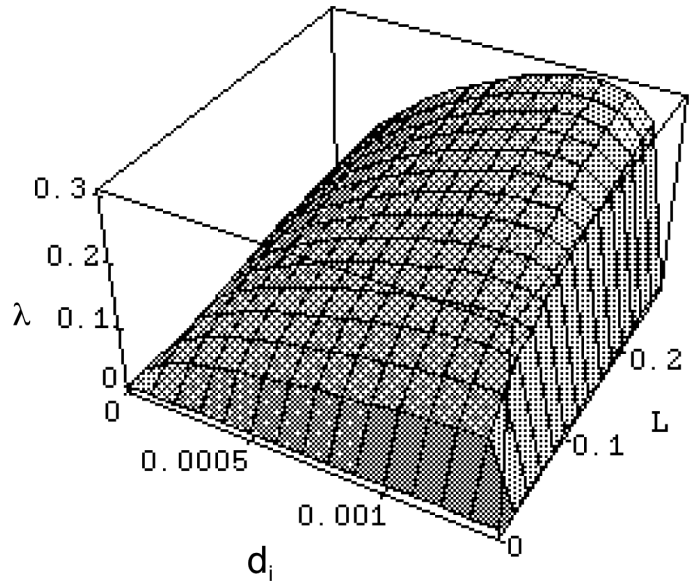

Fig. 4. Macroscopic space constant of the homogenized axon, λ, vs. the inner diameter, d_i, and internodal distance, L, for $d_o = 0.0014\,\text{cm}$ and $\delta = 0.00015\,\text{cm}$.

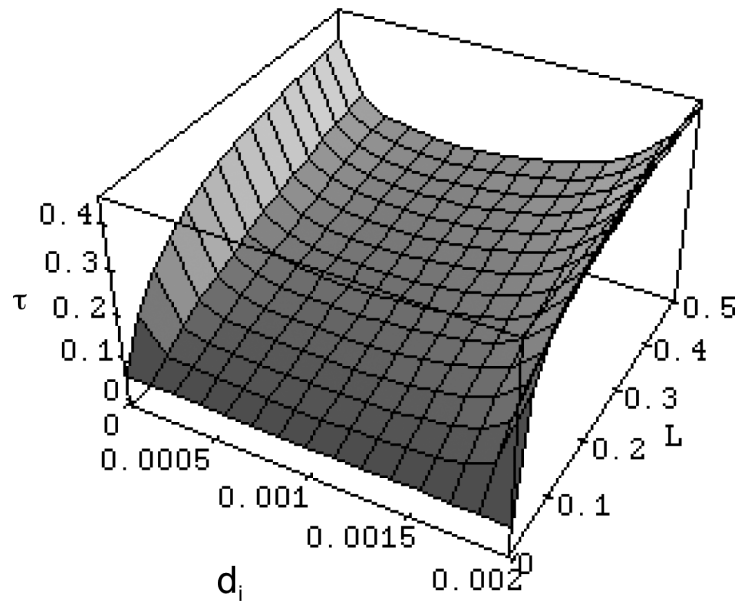

Fig. 5. Membrane time constant, τ, vs. internodal distance, L, and inner diameter, d_i, for $d_o = 0.0014\,\text{cm}$ and $\delta = 0.00015\,\text{cm}$. The time constant is a monotonically increasing function of L and exhibits a shallow minimum with respect to d_i.

note that τ is a monotonically increasing function of L but exhibits a minimum with respect to d_i for L constant. For $L = 100\,d_o$ the minimum occurs at $d_i/d_o = 0.367$ for $d_o = 0.0014\,\text{cm}$; $d_i/d_o = 0.1$ for $d_o = 0.0004\,\text{cm}$; and $d_i/d_o = 0.5$ for $d_o = 0.002\,\text{cm}$. In all physiological cases, the minimum in τ lies below $d_i/d_o = 0.606$. In addition, in the three limiting cases:

$$\lim_{d_i \to 0} \tau = \lim_{d_i \to do} \tau = \lim_{L \to \infty} \tau = \tau_m = 0.46\,\text{ms}. \tag{30}$$

A simple physical interpretation of the last limit is that the farther apart the nodes lie for a given outer diameter, the more the whole nerve resembles the myelinated segments and the more time it takes to charge the membrane.

It is then reasonable to speculate that one can derive the scaling relationships, Eqs. (28) and (29), by requiring that electrical disturbances attain the greatest spatial extent, λ, in the least time, τ. The simplest objective function is their ratio, c,

$$c = \frac{\lambda}{\tau}. \tag{31}$$

which has units of speed.

Although it is not meaningful to speak of a phase, group, or conduction velocity along a passive, lossy electrical cable, it is still possible to ascribe physical significance to c by studying physiologically relevant solutions to the macroscopic cable equation, Eq. (25). For example, it is possible to represent a nodal excitation as a step in transmembrane potential applied at $x = 0$ and $t = 0$. Then, the normalized transmembrane potential distribution, $V(x,t)$, is given as:

$$\begin{aligned} V(x,t) = \frac{1}{2}\exp\left(\frac{-|x|}{\lambda}\right)\left(1 - \text{erf}\left(\frac{|x|}{2\lambda}\sqrt{\frac{\tau}{t}} - \sqrt{\frac{t}{\tau}}\right)\right) \\ - \frac{1}{2}\exp\left(\frac{|x|}{\lambda}\right)\left(1 - \text{erf}\left(\frac{|x|}{2\lambda}\sqrt{\frac{\tau}{t}} + \sqrt{\frac{t}{\tau}}\right)\right) \end{aligned} \tag{32}$$

[21–23] where erf is the standard error function. Figure 6 depicts $V(x,t)$ as a function of x/λ and t/τ. Using Eq. (32), one can show that transmembrane potential reaches $0.635 \approx 1 - 1/e$ of its steady-state value at $t = \tau$ and $x = \lambda$. The same qualitative behavior is observed if a step in transmembrane current were applied at $x = 0$ and $t = 0$ [21, 22]. In these physiological cases, c can be interpreted as a characteristic speed of an electrical disturbance along the cable. By "characteristic speed" we simply mean the speed by which all disturbances can be scaled or normalized. Its use is not meant to conjure up the notion of a traveling wave, such as in the "method of characteristics". Figure 7 shows a plot of c as a function of d_i and L for $d_o = 0.0014\,\text{cm}$ and $\delta = 0.00015\,\text{cm}$. For all values of d_o in a physiological range, c exhibits a global maximum where the fractional change in λ equals the fractional change in τ. This is a simple consequence of logarithmic differentiation of c, i.e., $d\ln(c) = d\ln(\lambda) - d\ln(\tau) = 0$.

Rushton claimed that if the principle of corresponding states were true, then the nodal width should be constant, independent of axon size [1]. Constancy of nodal

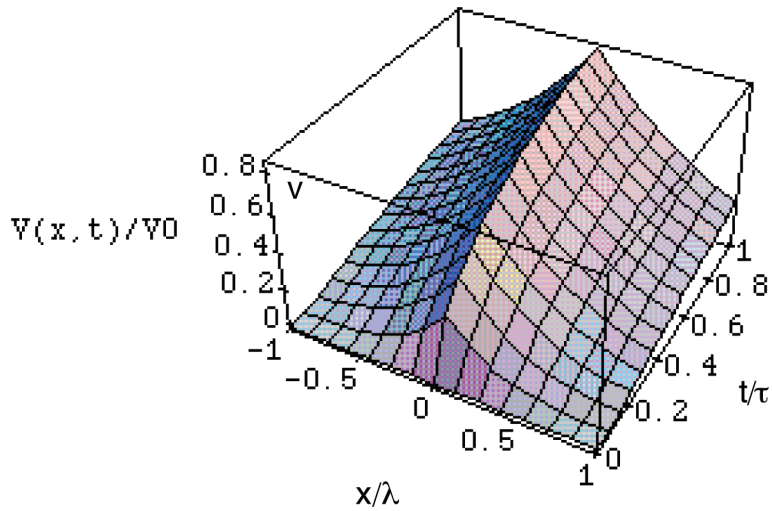

Fig. 6. Normalized transmembrane potential, $V(x,t)$, as a function of normalized axial distance, x/λ and time, t/τ calculated from Eq. (29).

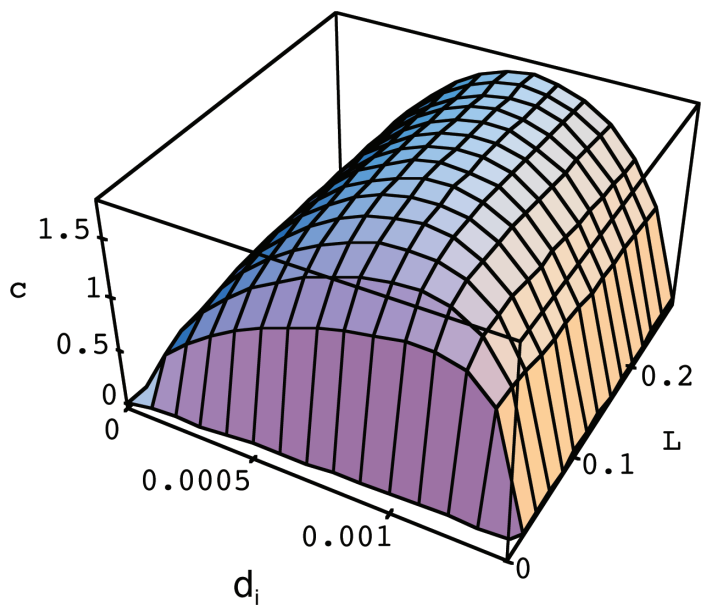

Fig. 7. Average speed, c, as a function of inner diameter, d_i, and internodal distance, L, for $d_o = 0.0014\,\text{cm}$ and $\delta = 0.00015\,\text{cm}$.

width δ is used here as a constraint in optimizing c. This is not unreasonable since the surrounding Schwann cell tightly regulates this dimension. The particular value of the node width that is used agrees with measurements of nodal capacitance per unit area made by Ritchie [20] and restated by Sweeney [24] for an axon whose outer

diameter is 0.0014 cm,

$$\delta = 0.00015\,\text{cm}. \tag{33}$$

Using Eq. (33) as a constraint equation, c is maximized using the method of Lagrange. The objective function, E, is written as a linear combination of c and the constraint equation:

$$E(d_i, d_o, L, \delta, \mu) = c(d_i, d_o, L, \delta) + \mu(\delta - 0.00015) \tag{34}$$

where μ is a Lagrange multiplier. For a particular outer diameter, d_o, the conditions for maximizing E are as follows:

$$\frac{\partial E}{\partial d_i} = \frac{\partial E}{\partial L} = \frac{\partial E}{\partial \delta} = \frac{\partial E}{\partial \mu} = 0. \tag{35}$$

These four non-linear simultaneous equations are solved numerically using Newton's method using values of d_o ranging from 0.0004 to 0.0020 cm.

For the set of variables, $\{d_i^{\text{opt}}, L^{\text{opt}}, \delta^{\text{opt}}, \mu^{\text{opt}}\}$, which solve Eq. (35) for a particular value of d_o, E attains a maximum when $d_i^{\text{opt}}/d_o = 0.604$. A plot of d_i^{opt} *vs.* d_o, given in Fig. 8, has a slope of 0.604. This calculated ratio is close to the value predicted by Rushton [1]. The optimal ratio of inner and outer diameters is fairly insensitive to changes in electrical parameters so, for instance, frog and rabbit nerve parameters produce the same value of d_i^{opt}/d_o.

The optimal ratio of internodal length and outer diameter, L^{opt}/d_o, however, is quite sensitive to the choice of material parameters. The objective function, E, attains a maximum when $L^{\text{opt}} = 97 d_o$ as shown in Fig. 9.

Although c does not represent the conduction velocity of an action potential along the axon, it also increases linearly with the axon's outer diameter [25].

It is also seen that the τ^{opt} (calculated from Eqs. (27) and (35)) is a constant, independent of d_o. This result follows directly from the constrained optimization of

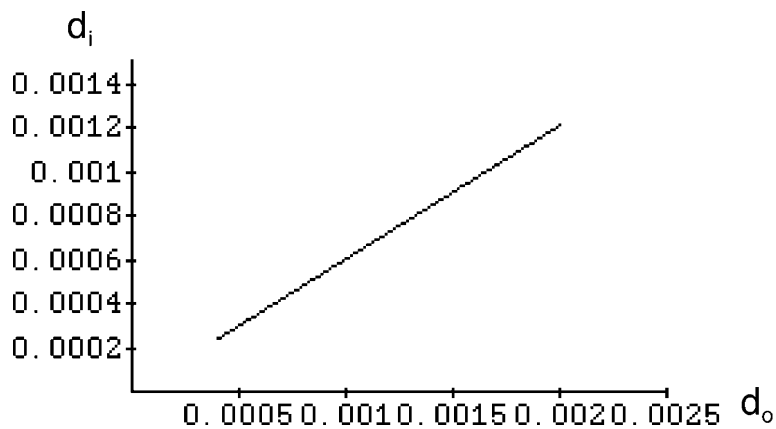

Fig. 8. Inner diameter, d_i vs. outer diameter, d_o, calculated numerically from Eq. (31). The slope of d_i vs. d_o is 0.6065.

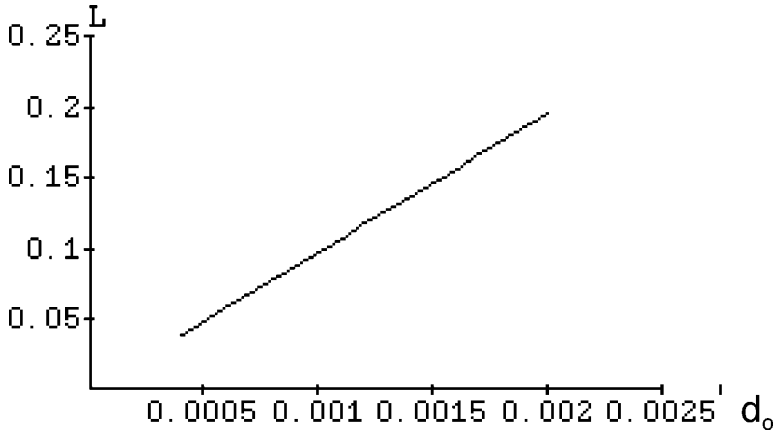

Fig. 9. The distance between nodes, L vs. outer diameter, d_o, predicted by a numerical solution of Eq. (31). A linear relation is predicted in which $L = 97d_o$.

c but it had to be assumed by Rushton as an axiom in the principle of corresponding states.

The success of the optimization method in obtaining many of Rushton's scaling results suggests that although energetic considerations may ultimately determine the width of the nodes and its channel density, once these quantities are prescribed, the remaining geometric relationships between inner and outer diameters and internodal length seem to be explained simply by maximizing the characteristic speed of transmission.

3.1. *Fault tolerance of the myelinated axon*

Using Eqs. (26) and (35), it can also be shown that $L^{\text{opt}}/\lambda^{\text{opt}}$ is independent of axon diameter, i.e.,

$$L^{\text{opt}} = 0.636\ \lambda^{\text{opt}} \approx (1 - 1/e)\lambda^{\text{opt}}. \tag{37}$$

This means that myelinated axons of all sizes should be equally fault tolerant. We can use this relation and Eq. (32) to predict how many inactive nodes must be placed adjacent to one another in order to block transmission of an action potential.

For a rabbit myelinated axon, the duration of the action potential is 3 ms, which is approximately 25 τ^{opt}. Therefore, the transmembrane potential distribution in Eq. (32) can be approximated by steady-state distribution. If an action potential were produced at the origin, $x = 0$, the transmembrane potential will have decayed by a factor of 0.5294 at $x = L$, by 0.28 at $x = 2L$, and by 0.148 at $x = 3L$, i.e.,

$$\lim_{t\to\infty} V(L,t) = 0.5294; \quad \lim_{t\to\infty} V(2L,t) = 0.280; \quad \lim_{t\to\infty} (3L,t) = 0.148.$$

If one node at $x = L$ were not excitable, the action potential at $x = 0$ would have to be at least 3.57 ($\geq 1/0.280$) times larger than threshold potential in order to stimulate the adjacent node at $x = 2L$. In rabbit myelinated axons, resting

potential ≈ -80 mV, peak transmembrane potential during depolarization $\approx$30 mV and threshold potential $\approx$30 mV [26]. Therefore, the peak amplitude of an action potential, 110 mV, is approximately 3.67 times larger than threshold potential, suggesting that a malfunctioning node located between two excitable nodes will not block conduction — a claim supported by Stämpfli [27].

However, an action potential is likely to be blocked by two (or more) adjacent inexcitable nodes. Stimulation of the nearest excitable node requires an action potential at least 6.75 ($\geq 1/0.148$) times larger than threshold potential. This prediction is supported by Tasaki's classical experiments [13]. This analysis also suggests the importance of the resting transmembrane potential and its contribution to the fault tolerance of the nerve.

The well-known advantage of this redundant design is that even if a particular node were inactive, the action potential could still jump to the next active node, allowing the nervous impulse to continue propagating along the axon. If we assume that the probability of a spontaneous failure of a node, p, is small ($say \sim 10^{-5}$), then the probability of failure of two consecutive nodes, assuming independence, would occur with probability p^2 ($\sim 10^{-10}$), which is much smaller than p.

4. Conclusions and Summary

Two important new developments are putting scaling principles in a new light. The first is that as our ability to control gene and protein expression increases, so does our ability to create mutants (e.g., knock-outs or knock-ins) whose nerve fibers have different dimensions, distribution of electrical properties and material composition, and micro and macro-architectures. It may be possible to perturb nerve properties in controlled ways and examine their functional consequences, and even to test whether these classical scaling laws are "optimal", for example, in terms of fault tolerance or maximizing the speed of information transfer along the axon.

Second, in this era of regenerative medicine, in which many are trying to coax the body to recapitulate events occurring in development to repair or regrow tissue, it is prudent to revisit classical scaling rules as a means to assess whether the new "engineered" tissue is competent to perform its intended function. For this purpose, it is important to have a conceptual framework with which to consider optimal performance of regenerated tissue. Having simple "engineering" principles in mind when "designing" or regenerating replacement nerve fibers is required for neural "tissue engineering" to live up to its name, i.e., to be a true engineering discipline.

Scaling arguments in biology are considered by some to be teleological. Here, no teleological reasoning or motives should be inferred. It is fair to say, however, that the design of nerve fibers according to the empirical rules discovered by Rushton and Tasaki are consistent with our notions of natural selection, i.e., neural architectures allowing nerves to perform their signal transmission functions optimally will likely be selected over sub-optimal designs during the course of evolution.

Finally, it is reasonable to extend this formalism to predict an optimal distribution of axon diameters within white matter fasciculi. A prudent starting point is that the optimal axon diameter distribution maximizes the channel capacity or rate of information transfer for a given total area of a fasciculus.

A macroscopic distributed cable equation has been derived from a continuum model of a myelinated axon using the two-space perturbation method. The macroscopic space and time constants of this simplified equation were used to derive two of Rushton's scaling rules by maximizing their ratio, the characteristic speed, while constraining the width of the node. Using this result, it was also possible to explain a well-known result about the fault tolerant behavior of myelinated axons. It should be noted that no free parameters were used in this analysis. Variables and physical constants used in these calculations were taken from published experimental data.

Acknowledgments

This work is dedicated to the memory of Gen Matsumoto who did so much to advance our understanding of the physics and physical chemistry of nervous excitation and brain organization. It is also dedicated to the memory of Nobuko Tasaki, wife of Ichiji Tasaki, a dear and valued member of our laboratory who passed away in 2003. Her kindness and warmth are sorely missed.

Thanks go to Richard Chadwick for interesting early discussions about Keller's method of multiple scales. Bradley Roth made thoughtful comments and provided much encouragement to publish this work, as did Seth Goldstein. The late Tom McMahon first introduced me to the principles of scaling and their applications to biology. Ichiji Tasaki made many useful observations and cogent criticisms of this work. Selma Gomez-Orr and Priya Gopalan proofread early versions of this manuscript with great care. Thanks also go to Liz Salak who edited this manuscript.

References

[1] Rushton WAH, A theory of the effects of fibre size in medullated nerve, *J Physiol (London)* **115**:101–122, 1951.

[2] FitzHugh R, Mathematical models of excitation and propagation in nerves, in Schwan H (ed.), *Biological Engineering*, McGraw-Hill: New York, pp. 1–83, 1969.

[3] Goldman L, Albus JS, Computation of impulse conduction in myelinated fibers: Theoretical basis of the velocity-diameter relation, *Biophys J* **8**:596–607, 1968.

[4] Keller JB, Darcy's law for flow in porous media and the two-space method, in Sternberg AJKRL, Papadakis JS (ed.), *Nonlinear Partial Equations in Engineering and Applied Science*, Marcel Dekker: New York, pp. 429–443, 1980.

[5] Guyton AC, *Textbook of Medical Physiology*, 6th ed., Philadelphia: W. B. Saunders, 1985.

[6] Waxman SG, Sadlow HA, The conduction properties of axons in central white matter, *Prog Neurobiol* **8**(4):297–324, 1977.

[7] Hallett M, Cohen LG, Magnetism: a new method for stimulation of nerve and brain, *JAMA* **262**:538–541, 1989.

[8] Rattay F, Analysis of models for external stimulation of axons, *IEEE Trans Biomed Eng* **33**:974–977, 1986.

[9] Basser PJ, Roth BJ, Stimulation of a myelinated nerve axon by electromagnetic induction, *Med Biol Eng Comput* **29**:261–268, 1991.

[10] Roth BJ, Cohen LG, Hallett M, The electric field induced during magnetic stimulation, *Electroencephalogr Clin Neurophysiol Suppl* **43**:268–278, 1991.

[11] Rattay F, Ways to approximate current-distance relations for electrically stimulated fibers, *J Theor Biol* **125**:339–349, 1987.

[12] Rattay F, Modeling the excitation of fibers under surface electrodes, *IEEE Trans Biomed Eng* **35**:199–202, 1988.

[13] Tasaki I, *Nervous Transmission*. Springfield, Illinois: Charles C. Thomas, 1953.

[14] Keller JB, Effective behavior of heterogeneous media, in Landman U (ed.), *Statistical Mechanics and Statistical Methods in Theory and Applications*, Plenum Press: New York, pp. 631–644, 1977.

[15] Basser PJ, Cable equation for a myelinated axon derived from its microstructure, *Med & Biol Eng Comput* **31**:S87–S92, 1993.

[16] Andrietti F, Bernardini G, Segmented and equivalent representation of the cable equation, *Biophys J* **46**:615–623, 1984.

[17] Basser PJ, Magnetic stimulation of peripheral axons: Models and experiments, in Ueno S (ed.), *Biomagnetic Stimulation*, Plenum Press: New York, pp. 119–129, 1994.

[18] FitzHugh R, Computation of impulse initiation and saltatory conduction in a myelinated nerve fiber, *Biophys J* **2**:11–21, 1962.

[19] Rattay F, Analysis of models for extracellular fiber stimulation, *IEEE Trans Biomed Eng* **36**:676–682, 1989.

[20] Ritchie JM, On the relation between fibre diameter and conduction velocity in myelinated nerve fibres, *Proc R Soc Lond B* **217**:29–35, 1982.

[21] Hodgkin AL, Rushton WAH, The electrical constants of a crustacean nerve fibre, *Proc Roy Soc Ser B* **130**:444–479, 1946.

[22] Plonsey R, *Bioelectric Phenomena*, McGraw-Hill: New York, 1969.

[23] Davis L Jr., Lorente deNó R, Contribution to the mathematical theory of electrotonus, *Stud Rockefeller Inst Med Res* **131**:442–496, 1947.

[24] Sweeney JD, Mortimer JT, Durand D, Modeling of mammalian myelinated nerve for functional neuromuscular stimulation, presented at *The 9th Annual Conference of IEEE EMBS*, 1987.

[25] Barr RC and Plonsey R, Electrophysiological interaction through the interstitial space between adjacent unmyelinated parallel fibers, *Biophys J* **61**:1164–1175, 1992.

[26] Chiu SY, Ritchie JM, Rogart RB, Stagg D, A quantitative description of membrane currents in rabbit myelinated nerve, *J Physiol (London)* **292**:149–166, 1979.

[27] Stämpfli R, Saltatory conduction in nerve, *Physiol Rev* **34**:101–111, 1954.